BIOCHEMISTRY

 Volume 43, Number 5 February 10, 2004

Current Topics

Structural Insights into Chloride and Proton-Mediated Gating of CLC Chloride Channels†

Michael Pusch*

Istituto di Biofisica, CNR, Via De Marini, 6, I-16149 Genova, Italy

Received November 6, 2003; Revised Manuscript Received December 15, 2003

ABSTRACT: CLC Cl^- channels fulfill numerous physiological functions as demonstrated by their involvement in several human genetic diseases. They have an unusual homodimeric architecture in which each subunit forms an individual pore whose open probability is regulated by various physicochemical factors, including voltage, Cl^- concentration, and pH. The voltage dependence of *Torpedo* channel CLC-0 is derived probably indirectly from the translocation of a Cl^- ion through the pore during the opening step. Recent structure determinations of bacterial CLC homologues marked a breakthrough for the structure−function analysis of CLC channels. The structures revealed a complex fold with 18 α-helices and two Cl^- ions per subunit bound in the center of the protein. The side chain of a highly conserved glutamate residue that resides in the putative permeation pathway appears to be a major component of the channel gate. First studies have begun to exploit the bacterial structures as guides for a rational structure−function analysis. These studies confirm that the overall structure seems to be conserved from bacteria to humans. A full understanding of the mechanisms of gating of eukaryotic CLC channels is, however, still lacking.

Physiological Functions of CLC Channels

CLC Cl^- channels form a nine-member gene family in mammals. CLC homologues are found in all eukaryotes and many prokaryotes (*1*). Most of the current knowledge about the physiological functions of mammalian CLCs has been gained from animal disease models, human genetic diseases, and knockout mice (*1*). The skeletal muscle specific channel CLC-1 is crucial for the stability of the resting membrane potential, and mutations in the CLCN1 gene can lead to dominant and recessive myotonia (*2*, *3*). CLC-2 is rather ubiquitously expressed (*4*), and CLC-2 knockout mice suggest a function in the ion homeostasis in testis and retina (*5*). Recently, the involvement of CLC-2 in human epilepsy was suggested (*6*). The kidney and inner ear specific channels, CLC-Ka and CLC-Kb (*7*−*9*), are probably involved in transepithelial Cl^- transport. Such a function is suggested by the fact that mutations of CLC-Kb lead to Bartter's syndrome, a salt wasting nephropathy (*10*), and by the CLC-Ka knockout phenotype that includes a strong nephrogenic diabetes insipidus (*11*). CLC-Ka and CLC-Kb channels are associated with a small β-subunit called barttin that is essential for proper functioning (*12*). Mutations in barttin lead to Bartter's syndrome which is associated with deafness (*13*).

The above-mentioned CLC channels fulfill their function in the plasma membrane, while the remaining mammalian CLC channels (CLC-3−7) are probably mostly important in mediating a Cl^- conductance in intracellular organelles such as endosomes and lysosomes. Here the Cl^- conductance

† This work was supported by a grant from the Italian Research Ministry (FIRB RBAU01PJMS).

* To whom correspondence should be addressed. Telephone: +39 0106475 561/522. Fax: +39 0106475 500. E-mail: pusch@ge.ibf.cnr.it.

10.1021/bi0359776 CCC: $27.50
Published on Web 01/09/2004

assists in an efficient acidification by a V-type H^+-ATPase, providing a path for charge compensating ion movement (*1*).

CLC-3−5 share a high degree of homology and display similar functional properties (*1*), even though some research groups claim that CLC-3 has very distinct properties and propose that CLC-3 is a swelling-activated channel located in the plasma membrane (*14*). Knockout mice of CLC-3, however, do not support this hypothesis (*15*, *16*). Mutations in the gene encoding CLC-5 lead to Dent's disease (*17*), a kidney disease that is characterized by low-molecular weight proteinurea, calciurea, and kidney stones. Results from CLC-5 knockout mice led to the model in which CLC-5 is located in early endosomes of the proximal tubule, where it is essential for the proper acidification of these vesicles (*18*, *19*).

CLC-4 has characteristics similar to those of CLC-5 in heterologous expression systems (*20*) and probably fulfills a similar physiological role (*21*). Almost nothing is known about the physiological role or functional properties of CLC-6. CLC-7 knockout mice display osteopetrosis and neurodegeneration (*22*), and mutations in the human CLCN7 gene can lead to recessive (*22*) and dominant osteopetrosis (*23*). The channel is probably localized to late endosomes and lysosomes and in the ruffled membranes of osteoclasts, the cells that reabsorb bone (*22*).

CLC channels have also been studied in model organisms such as *Caenorhabditis elegans* (*24*−*26*) and prokaryotes (*27*). The possible functions of CLC channels in *C. elegans* have recently been reviewed extensively (*28*). An understanding of the role and functional properties of CLC channels in prokaryotes is important because the available crystal structures have all been obtained from bacterial homologues (*29*, *30*). Unfortunately, bacterial CLCs can at present only be assayed in flux experiments but not in electrophysiological recordings (*31*).

This review will focus on the mechanisms of gating of CLC Cl^- channels. First, the phenotypic properties of CLC channels will be briefly summarized. Then the basic features of the recently determined X-ray structures of bacterial CLC proteins will be presented. Finally, the proposed mechanism of gating that resulted from the structural studies and future objectives of research will be discussed.

Functional Properties of CLC Channels

The prototype *Torpedo* CLC channel, CLC-0, is the best-studied channel from a functional and biophysical point of view. CLC-0 was discovered by Miller and colleagues who studied channel activity of the *Torpedo* electric organ in planar lipid bilayers (*32*). The most fascinating feature of the channel was its apparent two-pore architecture that manifested itself as two equidistant open conductance levels that open and close for quite long times practically independently of each other (Figure 1A). The presence of long shut periods, during which neither "protopore" conducts, demonstrated that the two conductance levels are tightly linked by a so-called common gate (Figure 1). These and other observations led Miller and colleagues to the proposal of the so-called double-barreled shotgun model (*33*). Jentsch and colleagues cloned CLC-0 in 1990 (*34*) and thus opened the way for the application of the powerful molecular biology tools. This led to the discovery of several new CLC homologues and allowed a biophysical analysis using heterologous expression systems. Finally, the recent high-yield purification and crystallization of prokaryotic CLCs represents another landmark in the exploration of CLC proteins (*29*−*31*). The crystal structures fully confirmed the double-barreled model. They revealed a very complex fold, with many more helices than previous studies predicted (*35*).

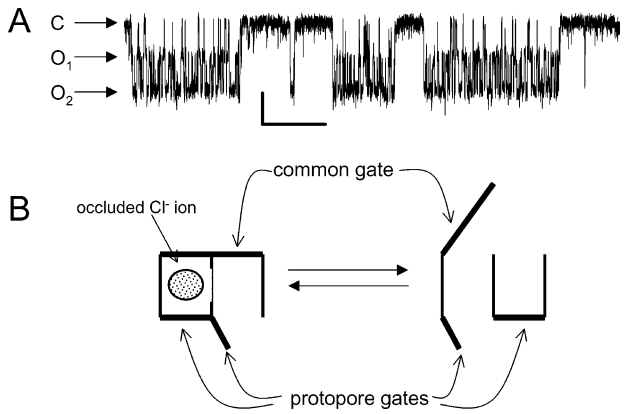

FIGURE 1: Double-barreled model of CLC-0. In panel A, a single-channel trace recorded from the CLC-0 point mutant I225M is shown to illustrate the "double-barreled" behavior. The mutant has faster kinetics of the common gate, facilitating its visualization (M. Pusch, unpublished result). C denotes the closed state, O_1 the current flowing if one protopore is open, and O_2 the current of two protopores. Several bursts are visible during which the two protopores fluctuate between open and closed states independently of each other. Scale bars indicate 2 s and 0.5 pA, respectively. The recording voltage was −80 mV. The trace is from an inside-out patch with symmetrical 100 mM Cl^-, filtered at 200 Hz. Panel B illustrates schematically the double-barreled structure with a common gate that acts on both protopores and an individual protopore gate for each protopore. If, as depicted in the cartoon, the two gates are physically separated and if they are on opposite ends of the channel, a state in which a Cl^- ion is occluded between the two gates as proposed by Richard and Miller (*42*) is possible.

Before these new structural insights are described in more detail, a brief description of the most important functional properties of some CLC channels will be provided. One of the goals of future structure−function studies will be to relate these functional properties to specific structures.

The open probability of all CLC channels studied so far depends on various physicochemical parameters, notably, voltage, Cl^- concentration, and pH. The phenotypes of all CLC channels that yielded functional expression in heterologous systems can be grossly divided into two groups. The first group includes *Torpedo* channel CLC-0 and human plasma membrane channels CLC-1, CLC-2, CLC-Ka, and CLC-Kb and their respective species homologues. Their gating is characterized by clear voltage- and Cl^--dependent relaxation kinetics. The other group includes CLC-3−5. These are extremely outwardly rectifying channels with no obvious Cl^--dependent gating relaxations in the time range of ≥5 ms (*20*, *36*−*38*). The rectification is possibly to a large extent a pore property; i.e., it reflects a single-channel rectification and not a gating relaxation (*39*). However, a detailed understanding of the gating and permeation properties of these channels is still missing. In particular, the single-channel gating behavior and the relationship of the functional properties and the double-pore architecture are not understood. These channels will thus not be considered further in this review. It must be kept in mind, however, that the

properties of the "CLC-3−5" group might resemble more closely those of the bacterial proteins than those of CLC-0 or CLC-1.

The total open probability of CLC-0 is governed by two different processes. One, the so-called fast gate, controls the aperture of the individual protopores, while the "slow gate" operates on both protopores simultaneously. The designations "fast" and "slow" derive from the vastly different time scales at which these gates change their state in the CLC-0 channel (Figure 1A). This purely kinetic distinction might be troublesome for other channels and also for mutants of CLC-0. I will call the two gates therefore the "protopore gate" and the "common gate", respectively. A large body of evidence demonstrates that the two protopore gates are completely independent from each other as long as the common gate is open (*33*, *40*, *41*). Nevertheless, the two types of gates, the protopore gate and the common gate, are not independent from each other. A striking demonstration of the coupling between the two gates was provided by Richard and Miller (*42*), who showed that the opening of the common gate is more likely if both protopore gates are open and that it closes more likely if only one or none of the protopore gates is open. This interdependence of the two gates is related to an inherently thermodynamically irreversible gating mechanism of CLC-0 (*42*): gating of CLC-0 is coupled to the electrochemical downhill flow of Cl^- ions. On the basis of a specific type of model, Miller and Richard (*42*) concluded that the two types of gates must be located on opposite sides of the channel, allowing the occlusion of a Cl^- ion between the two gates (Figure 1B). Later, it was shown that under conditions of a permanently open common gate the protopore gate itself is coupled to the movement of Cl^- ions through the channel. Most of the voltage dependence of the protopore gate is actually caused by the translocation of a Cl^- ion along the electric field across the membrane during the opening step (*43*). However, the open probability of the common gate also depends on the extracellular (*44*) as well as intracellular (*45*) Cl^- concentration, with a higher Cl^- concentration favoring gate aperture. In light of this quite complicated interdependence, the original observations of Richard and Miller (*42*) might not necessarily imply a state in which a Cl^- ion is occluded between the two gates. If there is no necessity for an occluded state, the two gates might also not be strictly physically separated as originally thought (*46*).

The protopore gate can be kinetically described as a simple two-state system

$$C \underset{\beta}{\overset{\alpha}{\rightleftharpoons}} O$$

with a voltage-dependent opening rate constant α and a closing rate constant β (*40*, *41*, *44*, *47*). The open probability is given by the relation $p_{open} = \alpha/(\alpha + \beta)$. While the open probability is an important gating property, a correlation of the gating mechanism(s) with defined conformational changes of the protein requires a clear distinction of the opening and closing rate constants.

As mentioned above, the opening of the protopore gate of CLC-0 appears to be a transition that is coupled to the translocation of a Cl^- ion across the channel during the actual opening step. The movement of Cl^- ions from the extracellular side to the inside during the Cl^--dependent opening

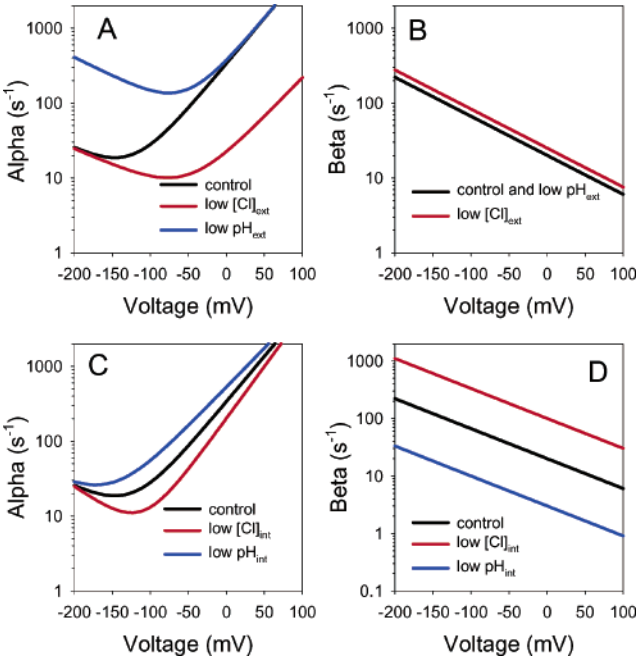

FIGURE 2: Dependence of the opening rate constant and closing rate constant of the protopore gate on extracellular and intracellular Cl^- concentration and pH. The opening rate constant (A and C) was calculated on the basis of the model of Chen and Miller (*44*), and the parameters were adjusted to illustrate qualitatively the effect of extracellular and intracellular Cl^- concentration and pH. The closing rate constant (B and D) was assumed to depend exponentially on voltage. The drawings are based on refs *40*, *44*, and *48*.

is favored at positive (inside) and disfavored at negative membrane voltages, and this provides the main source of the voltage dependence of the open probability. Experimentally it is, however, observed that the opening rate constant (α) exhibits a biphasic voltage dependence, with a minimum in the negative voltage range (*44*) (Figure 2A). To explain this behavior, Chen and Miller proposed that the protopore gate can reach the open conformation through an additional, Cl^--independent, transition with an increasing rate at hyperpolarized voltages (*44*).

A reduction in the extracellular Cl^- concentration has a strong effect on the opening rate (Figure 2A), while the closing rate constant (β) is only slightly affected (Figure 2B). The contrary is seen for changes in the intracellular Cl^- concentration: a reduction in $[Cl^-]_{int}$ strongly increases β, while α is less affected (Figure 2C,D).

The protopore gate also depends strongly on the extracellular and intracellular pH. A low pH, on either side, increases the open probability but apparently by quite different mechanisms for the two sides of the membrane. Changes in the intracellular pH shift the $p_{open}(V)$ curve across the voltage axis, while the extracellular pH mainly affects the minimal p_{open} at negative voltages. Hanke and Miller (*40*) concluded that a protonatable amino acid that is reached by protons from the inside changes its pK from ~6 to ~9 upon channel opening. Protonated protopores have an increased opening rate and a decreased closing rate. The effect of pH_{int} on the closing rate is similar to that of $[Cl^-]_{int}$ (Figure 2D).

This site of protonation from the inside seems to be different from that at which extracellular protons act because of the completely different effects on the opening versus closing rate constants. Protonation by extracellular protons

augments the opening rate constant by enhancing mostly the above-mentioned Cl^--independent, hyperpolarization-favored gating transition with little effect on the Cl^--dependent depolarization-favored opening transition. The closing rate constant was not found to be dependent on the extracellular pH (Figure 2A,B) (*48*). The apparent p*K* of the site accessible to extracellular protons was found to be around 5.3 (*48*). Via comparison of the effects of extracellular and intracellular Cl^- concentration and pH on the opening and closing rates, respectively (Figure 2), it seems that while the opening rate depends more strongly on extracellular factors, the closing rate is affected almost exclusively by intracellular Cl^- concentration and pH.

The quantitative properties of the common gate of CLC-0 are much less studied than those of the protopore gate. The reason is mainly that its kinetics are very slow, requiring very long recordings. In addition, the common gate is extremely temperature sensitive with a Q_{10} of the relaxation kinetics on the order of ~40 (*49*) requiring a precise temperature control of any quantitative measurement. An important aspect of the common gate is that it depends on the properties of both subunits of the channel. For example, the S123T mutant of CLC-0 strongly alters the quantitative properties of the common gate in homodimeric mutant channels. The alteration is dominantly conferred also to mutant−wild type (WT) heterodimers (*50*). Such a dominant effect of one (mutated) subunit on the properties of the common gate is also the basis of many dominant mutations of the gene encoding the muscle channel CLC-1 causing dominant myotonia (*3*, *51*−*54*). The large temperature dependence of the common gate suggests that it involves a major rearrangement of the protein dimer (*49*). In agreement with this speculation, mutations in many parts of the protein, probably including the cytoplasmic C-terminus, alter the properties of the common gate (*50*, *53*, *55*−*60*).

Gating of the muscle specific CLC-1 (*61*) is similar to that of the protopore gate of CLC-0 with regard to voltage (*43*, *54*, *61*−*65*), Cl^-, and pH dependence (*63*). The gating relaxations of CLC-1 are, however, more complex than those of CLC-0 (*63*), and its small single-channel conductance (*53*, *62*) makes a clear distinction between the protopore gate and the common gate difficult to elucidate. On the basis of several pieces of evidence, it was concluded that the fast component of CLC-1 gating corresponds mostly to the protopore gate while the slower component reflects mostly the common gate (*53*, *54*, *59*). The coupling between the two gates seems to be stronger than in CLC-0 (*54*).

Gating of other CLC channels is even less understood in terms of the double-barreled structure. The ubiquitous CLC-2 is activated slowly by hyperpolarizing voltages (*4*). When expressed in *Xenopus* oocytes, CLC-2 is in addition strongly activated by a reduction of the extracellular osmolarity (*66*). Voltage- and osmolarity-dependent gating involves the N-terminus of the channel (*66*) and the C-terminal half of helix J (*67*). In addition, CLC-2 gating depends on Cl^- concentration and pH (*45*, *67*, *68*), indicating that the underlying structural mechanisms are similar in CLC-0 and CLC-2. Like CLC-1 and CLC-2, the two "kidney" channels, CLC-Ka and CLC-Kb, are also ~40−50% identical to CLC-0 (*7*−*9*). The recent discovery that the CLC-K channels need an additional, structurally unrelated, β-subunit for an efficient plasma membrane expression (*12*) is, therefore, quite surprising. This additional two-transmembrane segment subunit is called barttin and was identified as the gene mutated in a variant of Bartter's syndrome associated with deafness (*13*). Coexpression of CLC-Ka or CLC-Ka with barttin leads to large Cl^- currents that are dependent on voltage and extracellular pH (*12*). An interesting feature of CLC-K channels, not shared by other CLC channels, is a strong dependence on the extracellular Ca^{2+} concentration (*12*, *69*).

Three channels, CLC-3−5, are highly homologous and have properties that are, however, very different from those of CLC-0−2, CLC-Ka, and CLC-Kb. They can be measured functionally at relatively low levels in heterologous expression systems (*20*, *36*, *37*). Currents are extremely outwardly rectifying with almost no measurable inward currents. This phenotype can, however, be changed by specific point mutations, as discussed below.

No currents have so far been reported for CLC-6 or CLC-7. It is therefore not even clear if these proteins are indeed Cl^- ion channels.

Structure of Bacterial CLC Channels

The first (and only) CLC structures were obtained from bacterial homologues (*29*). Pioneering work from the Miller lab showed that bacterial channels can be purified at high levels and functionally reconstituted (*31*). However, for the reconstituted bacterial protein, only Cl^- fluxes in vesicles could be detected, but no electrical activity was seen in lipid bilayers, suggesting a small single-channel conductance (*31*). The *Escherichia coli* CLC protein CLC-ec1 even spontaneously formed two-dimensional crystals that allowed the determination of a 6.5 Å resolution projection structure (*70*). X-ray structures were obtained initially from the *Salmonella typhimurium* channel at 3 Å resolution (*29*) and recently from *E. coli* at 2.5 Å in a cocrystallization with a monoclonal antibody (*30*). All the structures are very similar in the general architecture that displays a homodimeric channel in which each subunit has a triangular shape when viewed perpendicular to the membrane (Figure 3A). Cl^- ions were identified in the center of each subunit (Figure 3B,C), indicating that the likely pathways for the movement of the ions through the channel are ~40 Å from each other. This result unequivocally proves a double-barreled structure with two physically separated, independent, pores. In addition, the structure shows that each pore is entirely formed by a single subunit as anticipated from previous studies (*50*, *71*). The structure of each subunit of the CLC-ec1 protein is made up of 18 α-helices that are arranged in a complex fold with an unusual transmembrane topology. An interesting feature that emerged from the structure is that each subunit is itself a quasi-dimer with the sequences of the N-terminal half and the C-terminal half being significantly similar. The two halves are arranged in an inverted topology sandwiching around the central Cl^- ion (*29*, *30*). A similar inverted topology arrangement has also been observed in aquaporin H_2O channels that bear no apparent similarity in sequence to the Cl^- channel (*72*).

The most important functional property of an ion channel is to keep a balance between a selective discrimination of a certain ion species against others and the maintenance of a high transport rate. Strong ion binding by charged side chains

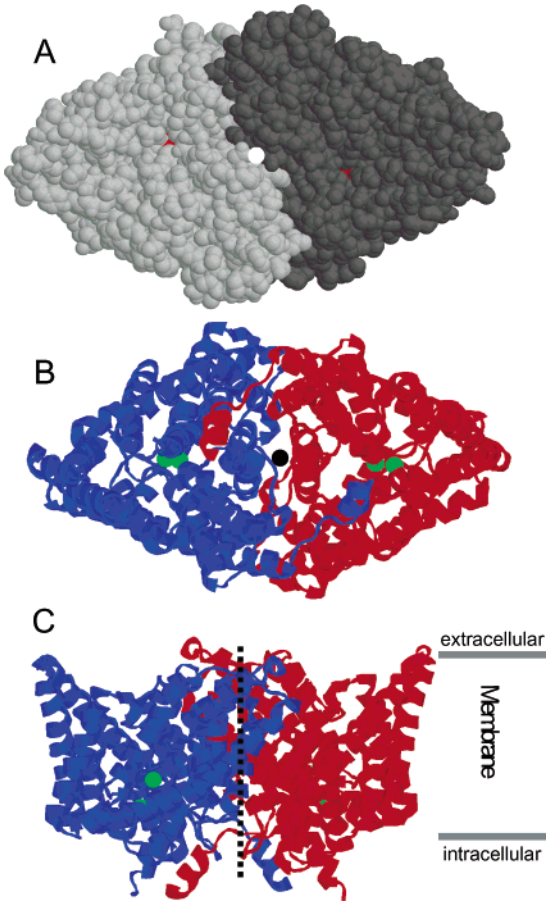

FIGURE 3: Overall architecture of the bacterial CLC protein CLC-ec1. In panel A, a space filling view of a homodimeric channel from the extracellular side is shown. One subunit is shown in light gray and the other in dark gray. The longest distance (i.e., from one "edge" to the other) is ~100 Å. For each subunit, Glu148 is colored red. The side chain of this glutamate appears to block the exit of a deeper Cl^- ion to the outside and marks the extracellular pore entrance. The two subunits of the dimer are related by an almost perfect 2-fold symmetry axis that is perpendicular to the plane of the drawing in panel A and represented by the white circle in the middle of the protein. In panel B, a view from the opposite, i.e., intracellular side, is shown illustrating the secondary structure that is all-α-helical. One subunit is shown in red and the other in blue. Two Cl^- ions (green) have been identified in each subunit. A black circle represents the 2-fold symmetry axis. In panel C, the position of the two Cl^- ions with respect to the (putative) location of the membrane is illustrated. The 2-fold symmetry axis is indicated by the dashed line. Drawings of the structures are all based on PDB entries 1OTS (for WT), 1OTT (E148A mutant), and 1OTU (E148Q mutant) from which the antibodies were removed. This figure was prepared with Rasmol (*89*).

would oppose fast permeation, while binding that was too loose would compromise ion selectivity. In CLC channels, this problem appears to be elegantly solved to a large extent by the complex arrangement of α-helices. Helices D, F, and N have their N-terminal ends pointing toward the crystallographically resolved central Cl^- binding site, stabilizing the negative charge with their positive dipole moment (Figure 4). The central Cl^- ion is further stabilized through interactions with the polar side chains of serine 107 and tyrosine 445 and with backbone amide groups from the loops preceding helices D, F, and N (*29*, *30*) (Figure 4). The protein segments surrounding the Cl^- binding sites are highly conserved among all CLC proteins, and some of the amino acids involved in ion binding had been previously identified

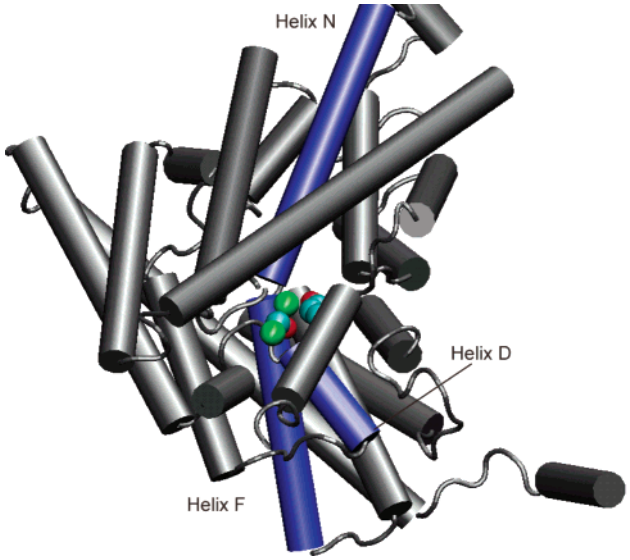

FIGURE 4: Helix dipole stabilization of Cl^- ions in the pore. The view is almost from the intracellular side. Helices are shown as cylinders. The two Cl^- ions are colored green. The N-terminal ends of helices D, F, and N (blue) point to the central Cl^- ion that makes additional contact with the side chains of residues S107 and Y445 that are shown in a space filling representation. The side chain of serine 107 is located exactly between the two Cl^- ions. This figure was prepared with VMD (*90*).

as pore residues using site-directed mutagenesis of CLC-0 and CLC-1 (see ref *1* for a review).

The ionic pore pathway is not immediately apparent in the CLC structure. The pore is not straight, but there seems to be a kink of the putative permeation pathway right in the center. Actually, the exit of the centrally bound Cl^- ion toward the extracellular space is clearly impeded by the side chain of a glutamate residue (E148) (Figures 3A and 5). Consequently, the glutamate residue was hypothesized to be a structural part of the protopore gate of the channel (*29*). Also, the exit toward the intracellular space seems to be severely hindered by the side chain of the highly conserved serine 107 (Figure 5). For these reasons, it has been assumed that the structure of the WT protein represents a closed, nonconducting conformation (*29*).

Even though bacterial channels are an interesting object of study on their own (*27*), an important question is the extent to which the structure of the bacterial protein can be applied to the mammalian homologues. Recent results from the Miller lab indicate that the bacterial protein may actually not be an ion channel but rather a transporter (A. Accardi and C. Miller, personal communication). Nevertheless, a recent study suggests a high degree of architectural conservation of CLC proteins from bacteria to humans (*73*). Estévez et al. identified several amino acids in regions that are distant in the primary sequence that strongly influence the action of small organic inhibitors 9-anthracenecarboxylic acid (9-AC) and *p*-chlorophenoxyacetic acid (CPA) on muscle channel CLC-1. When mapped onto the bacterial structure, the side chains of all high-impact residues cluster in a region close to the central Cl^- ion binding site while residues that have only small or no effect on inhibitor binding point away from those regions or are relatively far from the "high-impact" cluster (*73*). This result implies that the bacterial structure is adequate for guiding rational mutagenesis in exploring vertebrate CLC functions. Similarly, Chen's

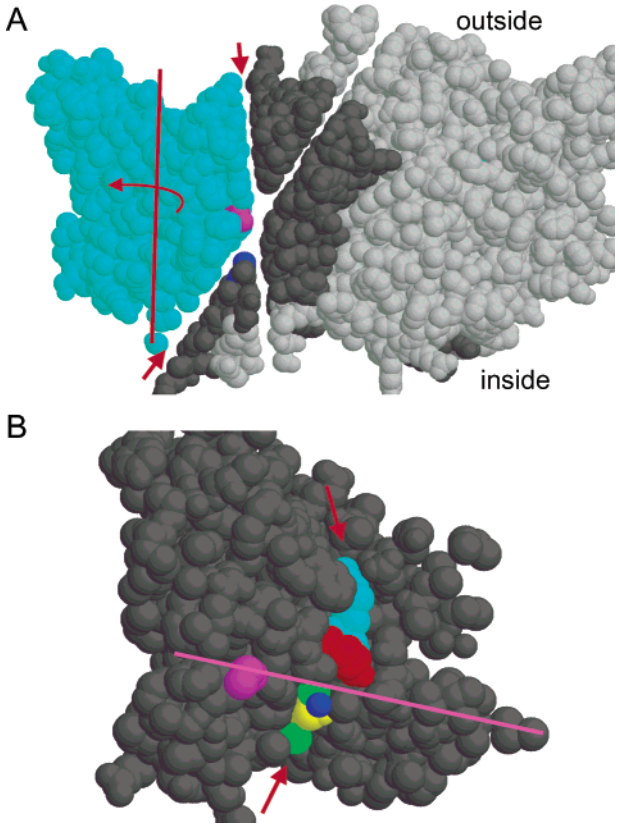

FIGURE 5: Putative permeation pathway. The figure shows both subunits in panel A. One subunit is colored dark gray and light blue and the other light gray. The view is laterally from the membrane with the intracellular side at the bottom. To illustrate the putative permeation pathway in one subunit, the protein was cut by two planes as indicated by the red arrows. The permeation pathway is approximately at the border of the light blue part of the protein along the cuts. In panel B, only the light blue part of the molecule in panel A is represented. The view in panel B is rotated with respect to that of panel A as indicated by the red line and the red arrow shown in panel A. Thus, one looks into the center of one monomer. To illustrate the relationship of the views in panels A and B, the same amino acid is colored pink in both panels (Leu397) and the edge created by the cuts shown in panel A is represented by a pink line in panel B. In panel B, Cl^- ions are colored green, serine 107 is colored yellow, glutamate 148 is colored red, and arginine 147 is colored light blue. Glutamate 148 blocks the exit of the central Cl^- ion toward the extracellular space, while serine 107 impedes the exit toward the inside. Tyrosine 445 is colored blue in both panels and is cut by the plane such that only the O atom of its side chain remains visible in panel B. This figure was prepared with Rasmol (*89*).

group concluded that the accessibility of intracellular structures of CLC-0 to cysteine reactive compounds corresponded to the expectations from the bacterial structures (*74*). From these studies, it is clear that the "higher-organism" CLC homologues must have a structure similar to those of the bacterial proteins. Nevertheless, the question of the level of detail of the bacterial channel that can be used to deduce precise functional properties of eukaryotic channels remains. Future studies comparing directly the functioning of the bacterial proteins in reconstitution systems to the X-ray structures will be extremely helpful in that respect.

One of the most intriguing features of the bacterial structure concerned the role of the "blocking" glutamate 148. From site-directed mutagenesis studies, an important role of this residue had already been somehow anticipated but never expressively interpreted (*20*, *35*, *75*, *76*). Furthermore, because mutations of the glutamate at most slightly changed ion selectivity (*76*), a pore location as found in the crystal structure was somewhat surprising. Recently, the role of the glutamate was investigated by Dutzler et al. (*30*) using X-ray crystallography of mutated channels. Dutzler et al. (*30*) resolved the structure of the E148A CLC-ec1 mutant, which lacks a bulky and deprotonatable side chain at position 148, and of E148Q, with a side chain at position 148 that approximates a protonated, electrically neutral, glutamate. Since at that time no functional electrophysiological assay for the bacterial protein had yet been established, Dutzler et al. analyzed the functional consequences of the corresponding mutations in *Torpedo* channel CLC-0. Both CLC-0 mutations, E166A and E166Q, showed the same phenotype of an almost complete loss of voltage dependence of gating being practically permanently open, like what is seen in CLC-1 (*35*, *73*, *75*). Also, the common gate becomes voltage-independent in the E166A mutant (M. Pusch, unpublished result). Surprisingly, the X-ray crystal structure of the mutants was very similar to that of the WT except for the localization of the side chain at position 148 (Figure 6). In the E148A mutant, a third Cl^- ion (in each protopore) was found in place of the carboxylate side chain in the WT structure (Figure 6A,B). Interestingly, the glutamine side chain in the E148Q mutant points toward the extracellular space, liberating the pore access, and a third Cl^- ion was found also here (Figure 6C). These spectacular structural results combined with the finding of the open phenotype of the corresponding mutations in CLC-0 led Dutzler et al. (*30*) to the conclusion that the protopore gating process of CLC-0 consists mainly of the movement of the negatively charged carboxylate group of the glutamate from a blocking position to a more extracellular orientation with little other conformational change. A further interesting finding was that CLC-0 currents at a low extracellular pH displayed a voltage-independent open phenotype, just like the E148Q mutation, consistent with the interpretation that the glutamate becomes protonated leading to an open channel just as in the mutant (*30*, *48*). The glutamate is therefore probably the residue that accounts for the extracellular pH dependence of CLC-0 gating (*48*).

From the structural data, thus, a simple model emerged for the mechanism of the fast protopore gate: extracellular Cl^- competes with the negatively charged side chain of Glu148 for a common binding site, leading to the strong Cl^- dependence of gating of CLC channels (*43*, *44*). The effect of extracellular pH on gating (*48*, *63*) is mediated by the protonation of Glu148 (Figure 7). In the following, this mechanism will be called the "glutamate-gating model".

While it is clear that the glutamate residue is fundamentally important for channel gating, several recently published papers argue somewhat against the simple picture in which gating consists only of the movement of its side chain. A first surprising result concerns the tyrosine that contributes the OH group of its side chain to the coordination of the central Cl^- ion. Mutating the corresponding residue in CLC-1 (*73*) or CLC-0 (*74*, *77*) to various residues, including phenylalanine, cysteine, and alanine, had only very minor effects on the single-channel conductance or selectivity properties. This is unexpected if the tyrosine is indeed coordinating the Cl^- ion in the open pore. Interestingly, the Y512F mutation quite drastically slowed the activation and

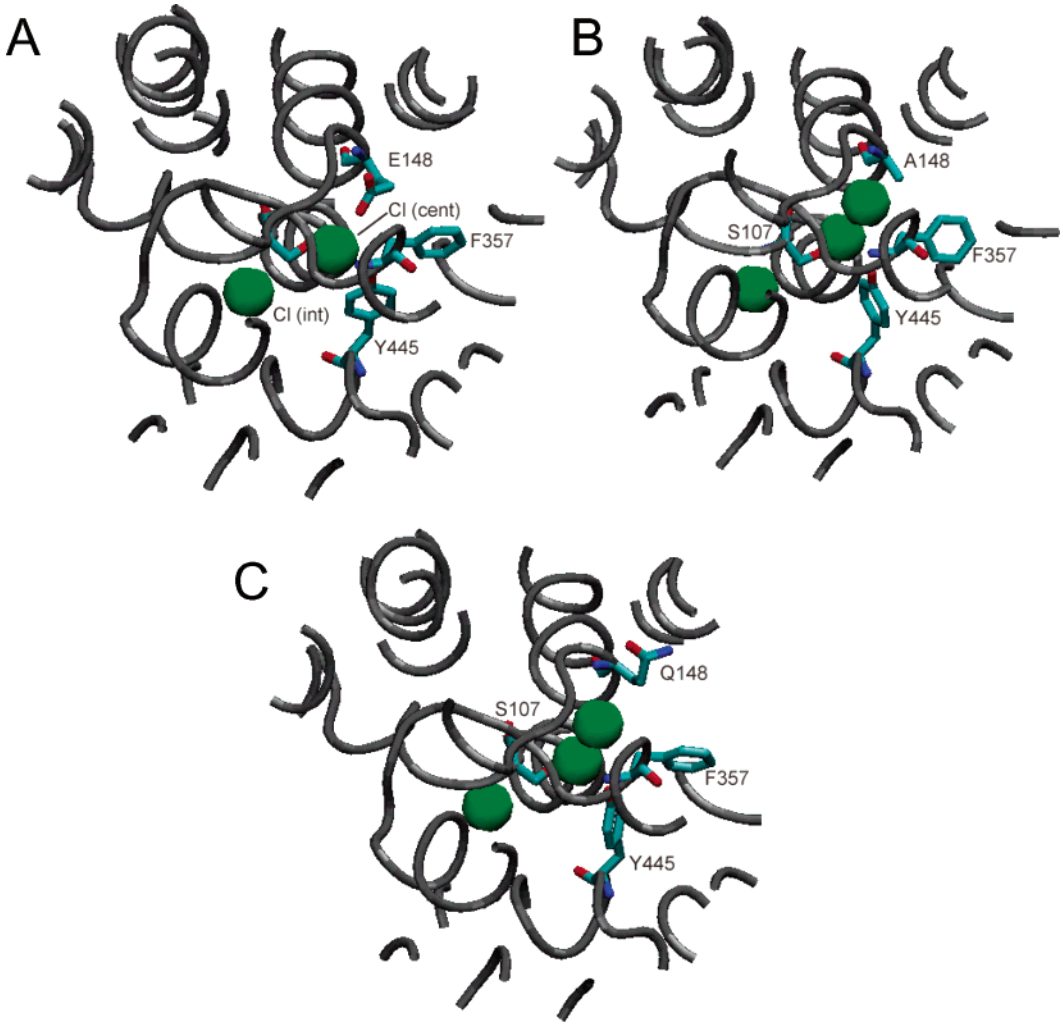

FIGURE 6: Putative open pore structures of mutated CLC-ec1 proteins. Parts of the structures of WT CLC-ec1 (A) and its E148A (B) and E148Q (C) mutants are shown according to the results of Dutzler et al. (*30*). Part of the protein that is within 13 Å of serine 107 is shown in each case with residues 107, 148, 357, and 445 shown explicitly. Note the presence of a third Cl^- in the two mutant structures at the position of the carboxylate side chain of E148 of WT. This figure was prepared with VMD (*90*).

deactivation kinetics of the CLC-0 protopore gate, suggesting a role of the tyrosine in gating (*77*).

Two recent studies used the small organic inhibitor CPA as a tool to test the predictions of the glutamate-gating model (*77*, *78*). Blocking of CLC-0 and CLC-1 by CPA and related compounds is highly state-dependent in that closed channels have a higher affinity than open channels (*47*, *77*, *79*). In terms of the glutamate-gating model, a higher closed state affinity for CPA has to be explained either by an indirect interaction of the blocker with pore resident Cl^- ions or by a direct interaction of CPA with the glutamate. An indication of the presence of conformational changes of the inner pore structure during protopore gating came from the differential effects of various pore mutations on the open and closed channel block by CPA (*77*). For example, the T471S mutation drastically increased the affinity for closed channels without altering the affinity for the open state, while the contrary happened with the Y512A mutation. These results suggest that other conformational rearrangements are taking place in CLC-0 in addition to the movement of the glutamate side chain. Traverso et al. (*78*) found that the constitutively open CLC-0 mutant E166A is strongly blocked by CPA with an affinity that is ~2000-fold larger than the open channel affinity of the WT. This is unexpected if the mutant represents a permanently open pore. For these reasons, Traverso et al. (*78*) proposed that the alanine mutant is still able to undergo a conformational change that resembles regular gating if the closed state is stabilized by CPA.

However, these above-mentioned results are indirectly based on functional measurements, and more rigorous tests of the glutamate-gating model involving additional structural data would be useful. In any case, a fundamental role of the glutamate residue for channel gating and pH sensitivity is clear. This is also true for other CLC channels, i.e., not only for CLC-0 or CLC-1: mutating the corresponding glutamate in CLC-3, CLC-4, or CLC-5 leads to profound changes in gating behavior (*20*, *80*).

How could the glutamate-gating model account for the Cl^- and pH dependence of the opening and closing rate constants of the protopore gate (Figure 2)? A dependence of the opening rate on $[Cl^-]_{ext}$ could be simply caused by a mechanism illustrated in Figure 7 (lower transition). When the glutamate side chain moves upward, its position is filled by a Cl^- ion coming from the extracellular space, preventing thereby an immediate closure. The movement of the Cl^- ion to this site could represent the voltage-dependent component

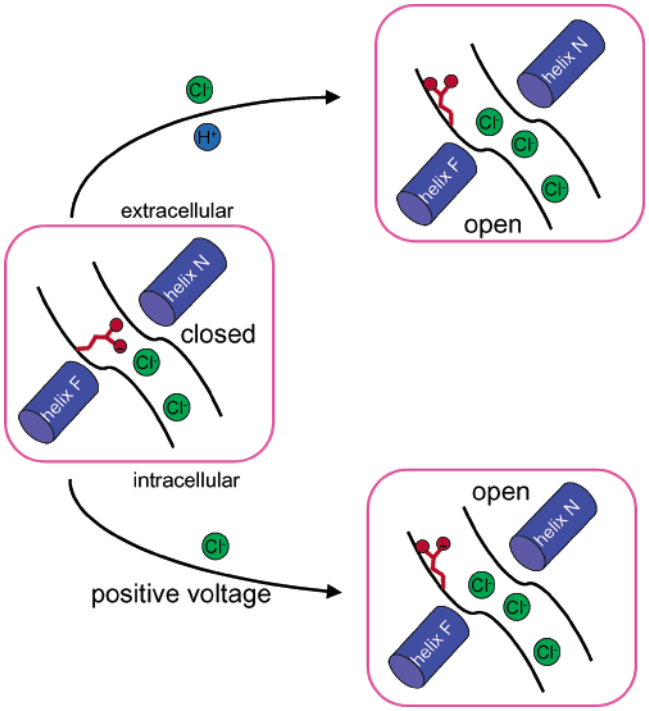

FIGURE 7: Glutamate-gating model. The pore of a closed channel (left) is blocked by the negatively charged side chain of glutamate 148. If Cl^- enters from the extracellular side, it can displace the glutamate. This process is supported by a positive voltage (lower transition). The glutamate can also be protonated by extracellular protons and then more easily displaced by a Cl^- ion (upper transition). This cartoon is an extreme oversimplification and highly speculative.

of the opening rate constant. However, Chen and Miller (*44*) have shown that the binding of extracellular Cl^- to the CLC-0 channel is intrinsically voltage-independent. It might thus be that the Cl^- is not directly arriving from the extracellular solution but from another, more extracellularly located binding site (that has yet to be identified) (*81*). In this picture, an intriguing possibility for explaining both the biphasic voltage dependence of the opening rate and the pH_{ext} dependence of the opening rate is the following. If the glutamate is protonated by an extracellular H^+ that travels about the same (electrical) distance as a Cl^-, and if the protonation event and the Cl^- binding event occur practically simultaneously, the effective electrical change in charge involved in this opening transition is small (Figure 7, upper transition). Such a process could account for the hyperpolarization-favored opening transition described by Chen and Miller (*44*).

Alternatively, it could also be that the outer site can be filled by a Cl^- coming from the central site, resulting in an inverted voltage dependence. The fact that only very small effects of $[Cl^-]_{int}$ on the opening rate constant have been found (*44*) (Figure 2) could be due to the high affinity of the central site such that the concentrations that have been used have not been sufficiently small.

It must be kept in mind that these considerations are extremely speculative. In light of this, an understanding of the Cl^- dependence of the closing rate is even more difficult because it requires a good understanding of the occupation probabilities of the various Cl^- binding sites in the open channel configuration. Such a detailed picture of the permeation process is not possible on the basis of the available data.

A major question regarding the glutamate-gating model is thus still whether the opening of a CLC-0 protopore requires additional conformational changes beyond those seen in the crystal structure of the mutated prokaryotic proteins.

Several additional important problems are not easily solved, even with the new structural data in hand. One concerns the basic mechanism of the common gate. Another question regards the role of the large cytoplasmic C-terminus that is found, for example, in all mammalian CLC channels. In particular, the C-terminus contains two so-called CBS domains (*82*), whose function is still obscure, that play an important role in CLC functioning (*1*, *22*, *83*−*88*). These CBS domains are absent from the prokaryotic channels whose structure has been resolved, and thus, nothing can be said right now about the kind of interaction with the transmembrane part of the protein.

Apart from the CBS domains, the C-termini of vertebrate and other CLC channels probably also contain various sorting and targeting signals that still must be identified, and in addition to barttin that appears to be specific for CLC-K channels, other interacting proteins likely exist and remain to be identified. The kind of interaction of barttin with CLC-K channels remains another open question that is also not easily answered using bacterial proteins as a model.

In summary, the determination of high-resolution structures of prokaryotic CLC proteins has opened exciting new perspectives for the elucidation of the mechanisms of functions of these fascinating proteins at a molecular level. Several important questions can now be approached in a rational manner, and the near future will certainly bring new surprises.

ACKNOWLEDGMENT

I thank Sonia Traverso and Alessio Accardi for critical comments on the manuscript.

REFERENCES

1. Jentsch, T. J., Stein, V., Weinreich, F., and Zdebik, A. A. (2002) Molecular structure and physiological function of chloride channels, *Physiol. Rev. 82*, 503−568.
2. Koch, M. C., Steinmeyer, K., Lorenz, C., Ricker, K., Wolf, F., Otto, M., Zoll, B., Lehmann-Horn, F., Grzeschik, K. H., and Jentsch, T. J. (1992) The skeletal muscle chloride channel in dominant and recessive human myotonia, *Science 257*, 797−800.
3. Pusch, M. (2002) Myotonia caused by mutations in the muscle chloride channel gene CLCN1, *Hum. Mutat. 19*, 423−434.
4. Thiemann, A., Gründer, S., Pusch, M., and Jentsch, T. J. (1992) A chloride channel widely expressed in epithelial and non-epithelial cells, *Nature 356*, 57−60.
5. Bösl, M. R., Stein, V., Hübner, C., Zdebik, A. A., Jordt, S. E., Mukhopadhyay, A. K., Davidoff, M. S., Holstein, A. F., and Jentsch, T. J. (2001) Male germ cells and photoreceptors, both dependent on close cell−cell interactions, degenerate upon ClC-2 Cl(−) channel disruption, *EMBO J. 20*, 1289−1299.
6. Haug, K., Warnstedt, M., Alekov, A. K., Sander, T., Ramirez, A., Poser, B., Maljevic, S., Hebeisen, S., Kubisch, C., Rebstock, J., Horvath, S., Hallmann, K., Dullinger, J. S., Rau, B., Haverkamp, F., Beyenburg, S., Schulz, H., Janz, D., Giese, B., Muller-Newen, G., Propping, P., Elger, C. E., Fahlke, C., Lerche, H., and Heils, A. (2003) Mutations in CLCN2 encoding a voltage-gated chloride channel are associated with idiopathic generalized epilepsies, *Nat. Genet. 33*, 527−532.
7. Uchida, S., Sasaki, S., Furukawa, T., Hiraoka, M., Imai, T., Hirata, Y., and Marumo, F. (1993) Molecular cloning of a

chloride channel that is regulated by dehydration and expressed predominantly in kidney medulla, *J. Biol. Chem. 268*, 3821−3824.
8. Kieferle, S., Fong, P., Bens, M., Vandewalle, A., and Jentsch, T. J. (1994) Two highly homologous members of the ClC chloride channel family in both rat and human kidney, *Proc. Natl. Acad. Sci. U.S.A. 91*, 6943−6947.
9. Adachi, S., Uchida, S., Ito, H., Hata, M., Hiroe, M., Marumo, F., and Sasaki, S. (1994) Two isoforms of a chloride channel predominantly expressed in thick ascending limb of Henle's loop and collecting ducts of rat kidney, *J. Biol. Chem. 269*, 17677−17683.
10. Simon, D. B., Bindra, R. S., Mansfield, T. A., Nelson-Williams, C., Mendonca, E., Stone, R., Schurman, S., Nayir, A., Alpay, H., Bakkaloglu, A., Rodriguez-Soriano, J., Morales, J. M., Sanjad, S. A., Taylor, C. M., Pilz, D., Brem, A., Trachtman, H., Griswold, W., Richard, G. A., John, E., and Lifton, R. P. (1997) Mutations in the chloride channel gene, CLCNKB, cause Bartter's syndrome type III, *Nat. Genet. 17*, 171−178.
11. Matsumura, Y., Uchida, S., Kondo, Y., Miyazaki, H., Ko, S. B., Hayama, A., Morimoto, T., Liu, W., Arisawa, M., Sasaki, S., and Marumo, F. (1999) Overt nephrogenic diabetes insipidus in mice lacking the CLC-K1 chloride channel, *Nat. Genet. 21*, 95−98.
12. Estévez, R., Boettger, T., Stein, V., Birkenhager, R., Otto, E., Hildebrandt, F., and Jentsch, T. J. (2001) Barttin is a Cl^- channel beta-subunit crucial for renal Cl^- reabsorption and inner ear K^+ secretion, *Nature 414*, 558−561.
13. Birkenhäger, R., Otto, E., Schurmann, M. J., Vollmer, M., Ruf, E. M., Maier-Lutz, I., Beekmann, F., Fekete, A., Omran, H., Feldmann, D., Milford, D. V., Jeck, N., Konrad, M., Landau, D., Knoers, N. V., Antignac, C., Sudbrak, R., Kispert, A., and Hildebrandt, F. (2001) Mutation of BSND causes Bartter syndrome with sensorineural deafness and kidney failure, *Nat. Genet. 29*, 310−314.
14. Duan, D., Winter, C., Cowley, S., Hume, J. R., and Horowitz, B. (1997) Molecular identification of a volume-regulated chloride channel, *Nature 390*, 417−421.
15. Stobrawa, S. M., Breiderhoff, T., Takamori, S., Engel, D., Schweizer, M., Zdebik, A. A., Bösl, M. R., Ruether, K., Jahn, H., Draguhn, A., Jahn, R., and Jentsch, T. J. (2001) Disruption of ClC-3, a chloride channel expressed on synaptic vesicles, leads to a loss of the hippocampus, *Neuron 29*, 185−196.
16. Arreola, J., Begenisich, T., Nehrke, K., Nguyen, H. V., Park, K., Richardson, L., Yang, B., Schutte, B. C., Lamb, F. S., and Melvin, J. E. (2002) Secretion and cell volume regulation by salivary acinar cells from mice lacking expression of the Clcn3 Cl^- channel gene, *J. Physiol. 545*, 207−216.
17. Fisher, S. E., Black, G. C., Lloyd, S. E., Hatchwell, E., Wrong, O., Thakker, R. V., and Craig, I. W. (1994) Isolation and partial characterization of a chloride channel gene which is expressed in kidney and is a candidate for Dent's disease (an X-linked hereditary nephrolithiasis), *Hum. Mol. Genet. 3*, 2053−2059.
18. Piwon, N., Günther, W., Schwake, M., Bösl, M. R., and Jentsch, T. J. (2000) ClC-5 Cl^--channel disruption impairs endocytosis in a mouse model for Dent's disease, *Nature 408*, 369−373.
19. Wang, S. S., Devuyst, O., Courtoy, P. J., Wang, X. T., Wang, H., Wang, Y., Thakker, R. V., Guggino, S., and Guggino, W. B. (2000) Mice lacking renal chloride channel, CLC-5, are a model for Dent's disease, a nephrolithiasis disorder associated with defective receptor-mediated endocytosis, *Hum. Mol. Genet. 9*, 2937−2945.
20. Friedrich, T., Breiderhoff, T., and Jentsch, T. J. (1999) Mutational analysis demonstrates that ClC-4 and ClC-5 directly mediate plasma membrane currents, *J. Biol. Chem. 274*, 896−902.
21. Mohammad-Panah, R., Harrison, R., Dhani, S., Ackerley, C., Huan, L. J., Wang, Y., and Bear, C. E. (2003) The chloride channel ClC-4 contributes to endosomal acidification and trafficking, *J. Biol. Chem. 278*, 29267−29277.
22. Kornak, U., Kasper, D., Bösl, M. R., Kaiser, E., Schweizer, M., Schulz, A., Friedrich, W., Delling, G., and Jentsch, T. J. (2001) Loss of the ClC-7 chloride channel leads to osteopetrosis in mice and man, *Cell 104*, 205−215.
23. Cleiren, E., Benichou, O., Van Hul, E., Gram, J., Bollerslev, J., Singer, F. R., Beaverson, K., Aledo, A., Whyte, M. P., Yoneyama, T., deVernejoul, M. C., and Van Hul, W. (2001) Albers-Schonberg disease (autosomal dominant osteopetrosis, type II) results from mutations in the ClCN7 chloride channel gene, *Hum. Mol. Genet. 10*, 2861−2867.
24. Schriever, A. M., Friedrich, T., Pusch, M., and Jentsch, T. J. (1999) CLC chloride channels in *Caenorhabditis elegans*, *J. Biol. Chem. 274*, 34238−34244.
25. Petalcorin, M. I., Oka, T., Koga, M., Ogura, K., Wada, Y., Ohshima, Y., and Futai, M. (1999) Disruption of clh-1, a chloride channel gene, results in a wider body of *Caenorhabditis elegans*, *J. Mol. Biol. 294*, 347−355.
26. Nehrke, K., Begenisich, T., Pilato, J., and Melvin, J. E. (2000) Into ion channel and transporter function. *Caenorhabditis elegans* ClC-type chloride channels: novel variants and functional expression, *Am. J. Physiol. 279*, C2052−C2066.
27. Iyer, R., Iverson, T. M., Accardi, A., and Miller, C. (2002) A biological role for prokaryotic ClC chloride channels, *Nature 419*, 715−718.
28. Strange, K. (2003) From genes to integrative physiology: ion channel and transporter biology in *Caenorhabditis elegans*, *Physiol. Rev. 83*, 377−415.
29. Dutzler, R., Campbell, E. B., Cadene, M., Chait, B. T., and MacKinnon, R. (2002) X-ray structure of a ClC chloride channel at 3.0 Å reveals the molecular basis of anion selectivity, *Nature 415*, 287−294.
30. Dutzler, R., Campbell, E. B., and MacKinnon, R. (2003) Gating the selectivity filter in ClC chloride channels, *Science 300*, 108−112.
31. Maduke, M., Pheasant, D. J., and Miller, C. (1999) High-level expression, functional reconstitution, and quaternary structure of a prokaryotic ClC-type chloride channel, *J. Gen. Physiol. 114*, 713−722.
32. Miller, C., and White, M. M. (1980) A voltage-dependent chloride conductance channel from Torpedo electroplax membrane, *Ann. N.Y. Acad. Sci. 341*, 534−551.
33. Miller, C. (1982) Open-state substructure of single chloride channels from Torpedo electroplax, *Philos. Trans. R. Soc. London, Ser. B 299*, 401−411.
34. Jentsch, T. J., Steinmeyer, K., and Schwarz, G. (1990) Primary structure of *Torpedo marmorata* chloride channel isolated by expression cloning in Xenopus oocytes, *Nature 348*, 510−514.
35. Schmidt-Rose, T., and Jentsch, T. J. (1997) Transmembrane topology of a CLC chloride channel, *Proc. Natl. Acad. Sci. U.S.A. 94*, 7633−7638.
36. Steinmeyer, K., Schwappach, B., Bens, M., Vandewalle, A., and Jentsch, T. J. (1995) Cloning and functional expression of rat CLC-5, a chloride channel related to kidney disease, *J. Biol. Chem. 270*, 31172−31177.
37. Li, X., Shimada, K., Showalter, L. A., and Weinman, S. A. (2000) Biophysical properties of ClC-3 differentiate it from swelling-activated chloride channels in Chinese hamster ovary-K1 cells, *J. Biol. Chem. 275*, 35994−35998.
38. Vanoye, C. G., and George, A. L., Jr. (2002) Functional characterization of recombinant human ClC-4 chloride channels in cultured mammalian cells, *J. Physiol. 539*, 373−383.
39. Hebeisen, S., Heidtmann, H., Cosmelli, D., Gonzalez, C., Poser, B., Latorre, R., Alvarez, O., and Fahlke, C. (2003) Anion Permeation in Human ClC-4 Channels, *Biophys. J. 84*, 2306−2318.
40. Hanke, W., and Miller, C. (1983) Single chloride channels from Torpedo electroplax. Activation by protons, *J. Gen. Physiol. 82*, 25−45.
41. Ludewig, U., Pusch, M., and Jentsch, T. J. (1997) Independent gating of single pores in CLC-0 chloride channels, *Biophys. J. 73*, 789−797.
42. Richard, E. A., and Miller, C. (1990) Steady-state coupling of ion-channel conformations to a transmembrane ion gradient, *Science 247*, 1208−1210.
43. Pusch, M., Ludewig, U., Rehfeldt, A., and Jentsch, T. J. (1995) Gating of the voltage-dependent chloride channel CIC-0 by the permeant anion, *Nature 373*, 527−531.
44. Chen, T. Y., and Miller, C. (1996) Nonequilibrium gating and voltage dependence of the ClC-0 Cl^- channel, *J. Gen. Physiol. 108*, 237−250.
45. Pusch, M., Jordt, S. E., Stein, V., and Jentsch, T. J. (1999) Chloride dependence of hyperpolarization-activated chloride channel gates, *J. Physiol. 515*, 341−353.
46. Miller, C., and Richard, E. A. (1990) in *Chloride Channels and Carriers in Nerve, Muscle and Glial Cells* (Alvarez-Leefmans, F. J., and Russell, J. M., Eds.) pp 383−405, Plenum, New York.
47. Pusch, M., Accardi, A., Liantonio, A., Ferrera, L., De Luca, A., Camerino, D. C., and Conti, F. (2001) Mechanism of block of

single protopores of the Torpedo chloride channel ClC-0 by 2-(*p*-chlorophenoxy)butyric acid (CPB), *J. Gen. Physiol. 118*, 45−62.
48. Chen, M. F., and Chen, T. Y. (2001) Different fast-gate regulation by external Cl(−) and H(+) of the muscle-type ClC chloride channels, *J. Gen. Physiol. 118*, 23−32.
49. Pusch, M., Ludewig, U., and Jentsch, T. J. (1997) Temperature dependence of fast and slow gating relaxations of ClC-0 chloride channels, *J. Gen. Physiol. 109*, 105−116.
50. Ludewig, U., Pusch, M., and Jentsch, T. J. (1996) Two physically distinct pores in the dimeric ClC-0 chloride channel, *Nature 383*, 340−343.
51. Pusch, M., Steinmeyer, K., Koch, M. C., and Jentsch, T. J. (1995) Mutations in dominant human myotonia congenita drastically alter the voltage dependence of the CIC-1 chloride channel, *Neuron 15*, 1455−1463.
52. Plassart-Schiess, E., Gervais, A., Eymard, B., Lagueny, A., Pouget, J., Warter, J. M., Fardeau, M., Jentsch, T. J., and Fontaine, B. (1998) Novel muscle chloride channel (CLCN1) mutations in myotonia congenita with various modes of inheritance including incomplete dominance and penetrance, *Neurology 50*, 1176−1179.
53. Saviane, C., Conti, F., and Pusch, M. (1999) The muscle chloride channel ClC-1 has a double-barreled appearance that is differentially affected in dominant and recessive myotonia, *J. Gen. Physiol. 113*, 457−468.
54. Accardi, A., and Pusch, M. (2000) Fast and slow gating relaxations in the muscle chloride channel CLC-1, *J. Gen. Physiol. 116*, 433−444.
55. Ludewig, U., Jentsch, T. J., and Pusch, M. (1997) Inward rectification in ClC-0 chloride channels caused by mutations in several protein regions, *J. Gen. Physiol. 110*, 165−171.
56. Ludewig, U., Jentsch, T. J., and Pusch, M. (1997) Analysis of a protein region involved in permeation and gating of the voltage-gated Torpedo chloride channel ClC-0, *J. Physiol. 498*, 691−702.
57. Fong, P., Rehfeldt, A., and Jentsch, T. J. (1998) Determinants of slow gating in ClC-0, the voltage-gated chloride channel of *Torpedo marmorata*, *Am. J. Physiol. 274*, C966−C973.
58. Lin, Y. W., Lin, C. W., and Chen, T. Y. (1999) Elimination of the slow gating of ClC-0 chloride channel by a point mutation, *J. Gen. Physiol. 114*, 1−12.
59. Accardi, A., Ferrera, L., and Pusch, M. (2001) Drastic reduction of the slow gate of human muscle chloride channel (ClC-1) by mutation C277S, *J. Physiol. 534*, 745−752.
60. Duffield, M., Rychkov, G., Bretag, A., and Roberts, M. (2003) Involvement of Helices at the Dimer Interface in ClC-1 Common Gating, *J. Gen. Physiol. 121*, 149−161.
61. Steinmeyer, K., Ortland, C., and Jentsch, T. J. (1991) Primary structure and functional expression of a developmentally regulated skeletal muscle chloride channel, *Nature 354*, 301−304.
62. Pusch, M., Steinmeyer, K., and Jentsch, T. J. (1994) Low single channel conductance of the major skeletal muscle chloride channel, ClC-1, *Biophys. J. 66*, 149−152.
63. Rychkov, G. Y., Pusch, M., Astill, D. S., Roberts, M. L., Jentsch, T. J., and Bretag, A. H. (1996) Concentration and pH dependence of skeletal muscle chloride channel ClC-1, *J. Physiol. 497*, 423−435.
64. Rychkov, G. Y., Pusch, M., Roberts, M. L., Jentsch, T. J., and Bretag, A. H. (1998) Permeation and block of the skeletal muscle chloride channel, ClC-1, by foreign anions, *J. Gen. Physiol. 111*, 653−665.
65. Rychkov, G., Pusch, M., Roberts, M., and Bretag, A. (2001) Interaction of hydrophobic anions with the rat skeletal muscle chloride channel ClC-1: effects on permeation and gating, *J. Physiol. 530*, 379−393.
66. Gründer, S., Thiemann, A., Pusch, M., and Jentsch, T. J. (1992) Regions involved in the opening of CIC-2 chloride channel by voltage and cell volume, *Nature 360*, 759−762.
67. Jordt, S. E., and Jentsch, T. J. (1997) Molecular dissection of gating in the ClC-2 chloride channel, *EMBO J. 16*, 1582−1592.
68. Arreola, J., Begenisich, T., and Melvin, J. E. (2002) Conformation-dependent regulation of inward rectifier chloride channel gating by extracellular protons, *J. Physiol. 541*, 103−112.
69. Uchida, S., Sasaki, S., Nitta, K., Uchida, K., Horita, S., Nihei, H., and Marumo, F. (1995) Localization and functional characterization of rat kidney-specific chloride channel, ClC-K1, *J. Clin. Invest. 95*, 104−113.
70. Mindell, J. A., Maduke, M., Miller, C., and Grigorieff, N. (2001) Projection structure of a ClC-type chloride channel at 6.5 Å resolution, *Nature 409*, 219−223.
71. Weinreich, F., and Jentsch, T. J. (2001) Pores formed by single subunits in mixed dimers of different CLC chloride channels, *J. Biol. Chem. 276*, 2347−2353.
72. Stroud, R. M., Miercke, L. J., O'Connell, J., Khademi, S., Lee, J. K., Remis, J., Harries, W., Robles, Y., and Akhavan, D. (2003) Glycerol facilitator GlpF and the associated aquaporin family of channels, *Curr. Opin. Struct. Biol. 13*, 424−431.
73. Estévez, R., Schroeder, B. C., Accardi, A., Jentsch, T. J., and Pusch, M. (2003) Conservation of Chloride Channel Structure Revealed by an Inhibitor Binding Site in ClC-1, *Neuron 38*, 47−59.
74. Lin, C. W., and Chen, T. Y. (2003) Probing the pore of ClC-0 by substituted cysteine accessibility method using methane thiosulfonate reagents, *J. Gen. Physiol. 122*, 147−159.
75. Fahlke, C., Yu, H. T., Beck, C. L., Rhodes, T. H., and George, A. L., Jr. (1997) Pore-forming segments in voltage-gated chloride channels, *Nature 390*, 529−532.
76. Waldegger, S., and Jentsch, T. J. (2000) Functional and structural analysis of ClC-K chloride channels involved in renal disease, *J. Biol. Chem. 275*, 24527−24533.
77. Accardi, A., and Pusch, M. (2003) Conformational changes in the pore of CLC-0, *J. Gen. Physiol. 122*, 277−293.
78. Traverso, S., Elia, L., and Pusch, M. (2003) Gating competence of constitutively open CLC-0 mutants revealed by the interaction with a small organic inhibitor, *J. Gen. Physiol. 122*, 295−306.
79. Pusch, M., Accardi, A., Liantonio, A., Guida, P., Traverso, S., Camerino, D. C., and Conti, F. (2002) Mechanisms of block of muscle type CLC chloride channels, *Mol. Membr. Biol. 19*, 285−292.
80. Li, X., Wang, T., Zhao, Z., and Weinman, S. A. (2002) The ClC-3 chloride channel promotes acidification of lysosomes in CHO-K1 and Huh-7 cells, *Am. J. Physiol. 282*, C1483−C1491.
81. Pusch, M. (1996) Knocking on channel's door. The permeating chloride ion acts as the gating charge in ClC-0, *J. Gen. Physiol. 108*, 233−236.
82. Ponting, C. P. (1997) CBS domains in CIC chloride channels implicated in myotonia and nephrolithiasis (kidney stones), *J. Mol. Med. 75*, 160−163.
83. Schmidt-Rose, T., and Jentsch, T. J. (1997) Reconstitution of functional voltage-gated chloride channels from complementary fragments of CLC-1, *J. Biol. Chem. 272*, 20515−20521.
84. Hryciw, D. H., Rychkov, G. Y., Hughes, B. P., and Bretag, A. H. (1998) Relevance of the D13 region to the function of the skeletal muscle chloride channel, ClC-1, *J. Biol. Chem. 273*, 4304−4307.
85. Maduke, M., Williams, C., and Miller, C. (1998) Formation of CLC-0 chloride channels from separated transmembrane and cytoplasmic domains, *Biochemistry 37*, 1315−1321.
86. Schwappach, B., Stobrawa, S., Hechenberger, M., Steinmeyer, K., and Jentsch, T. J. (1998) Golgi localization and functionally important domains in the NH2 and COOH terminus of the yeast CLC putative chloride channel Gef1p, *J. Biol. Chem. 273*, 15110−15118.
87. Estévez, R., and Jentsch, T. J. (2002) CLC chloride channels: correlating structure with function, *Curr. Opin. Struct. Biol. 12*, 531−539.
88. Carr, G., Simmons, N., and Sayer, J. (2003) A role for CBS domain 2 in trafficking of chloride channel CLC-5, *Biochem. Biophys. Res. Commun. 310*, 600−605.
89. Sayle, R. A., and Milner-White, E. J. (1995) RASMOL: biomolecular graphics for all, *Trends Biochem. Sci. 20* 374.
90. Humphrey, W., Dalke, A., and Schulten, K. (1996) VMD: visual molecular dynamics, *J. Mol. Graphics 14*, 27−28.

BI0359776